Non-Fermi-Liquid Single Particle Line Shape of the Quasi-One-Dimensional Non-CDW Metal $Li_{0.9}Mo_6O_{17}$: Comparison to the Luttinger Liquid

J. D. Denlinger,[1] G.-H. Gweon,[1] J. W. Allen,[1] C. G. Olson,[2] J. Marcus,[3] C. Schlenker,[1] and L.-S. Hsu[1,*]

[1]*Randall Laboratory of Physics, University of Michigan, Ann Arbor, Michigan 48109-1120*

[2]*Ames Laboratory, Iowa State University, Ames, Iowa 50011*

[3]*Laboratoire d'Etudes des Propriétés Electroniques des Solides–CNRS, BP166, 38042 Grenoble Cedex, France*

(Received 11 September 1998)

We report the detailed non-Fermi-liquid (NFL) line shape of the dispersing excitation which defines the Fermi surface for quasi-one-dimensional $Li_{0.9}Mo_6O_{17}$. The properties of $Li_{0.9}Mo_6O_{17}$ strongly suggest that the NFL behavior has a purely electronic origin. In relation to the theoretical Luttinger liquid line shape, we identify significant similarities, but also important differences. [S0031-9007(99)08752-9]

PACS numbers: 71.10.Pm, 71.18.+y, 79.60.–i

A topic of high current interest and fundamental importance for condensed matter physics is the possible failure due to electron-electron interactions [1] of the Fermi-liquid paradigm for metals. The paradigm lattice non-Fermi-liquid (NFL) scenario for a metal is the Luttinger liquid (LL) behavior [2] of an interacting one-dimensional electron gas. The energy (ω) and momentum ($\mathbf{k}$) resolved single particle spectral function $A(\mathbf{k},\omega)$ for the dispersing excitation that defines the Fermi surface (FS) is much different for the LL than for a Fermi liquid [3,4]. Since $A(\mathbf{k},\omega)$ can be measured by angle-resolved photoemission spectroscopy (ARPES), there has been strong motivation for such studies of quasi-one-dimensional (q-1D) metals. An unfortunate complication for this line of research is that many q-1D metals display charge density wave (CDW) formation and that strong CDW fluctuations involving electron-phonon interactions above the CDW transition temperature can also cause $A(\mathbf{k},\omega)$ to have NFL behavior which in some ways resembles that of the LL [5,6]. For example, both scenarios predict a substantial suppression of $\mathbf{k}$-integrated spectral weight near E_F, bringing ambiguity to the interpretation of pioneering angle integrated photoemission measurements [7,8] which observed such a weight suppression, and to subsequent ARPES studies [9,10] of dispersing line shapes in q-1D CDW materials.

Thus far ARPES studies of non-CDW q-1D metals have not obtained dispersing line shape data which could be compared meaningfully with many-body theories. Most of the non-CDW q-1D metals are organic and for these metals $\mathbf{k}$-integrated weight suppression near E_F occurs [8], but dispersing features have not been observed [11]. $Li_{0.9}Mo_6O_{17}$ is a 3D material with bonding such that only q-1D bands define its FS. It is unusual as a q-1D inorganic metal which appears to be free of strong electron-phonon effects, as discussed further below, and which shows suppressed E_F photoemission weight. An initial ARPES study [12] at 300 K did not resolve individual valence band features but did observe for a single broad peak a general angle dependent shift and diminution of spectral weight which enabled a q-1D FS to be deduced. A second study [10] obtained similar data. A third study [13] resolved valence band structure but the peak dispersing to E_F was too weak in the spectra for its line shape to be discerned.

Here we report the detailed NFL line shape of the dispersing excitation which defines the FS for $Li_{0.9}Mo_6O_{17}$. Obtaining the line shape data was enabled by taking precautions to minimize photon-induced sample damage [14] and by studying a region in $\mathbf{k}$ space where the near-E_F ARPES intensity is especially large, as determined by first making a $\mathbf{k}$-space map of the ARPES intensity near E_F. The properties of $Li_{0.9}Mo_6O_{17}$ strongly argue that the NFL behavior has a purely electronic origin, giving this set of data a special current importance. $Li_{0.9}Mo_6O_{17}$ displays metallic T-linear resistivity ρ and temperature independent magnetic susceptibility χ for temperatures down to $T_X \approx 24$ K, where a phase transition of unknown origin is signaled by a very weak anomaly in the specific heat [15]. As T decreases below T_X, ρ increases, but χ is unchanged [15,16]. Most significant, infrared optical studies which routinely detect CDW or spin density wave (SDW) gaps [17] in other materials, do not show any gap opening [18] for energies down to 1 meV, setting an upper limit of $(11.6/3.52) \approx 3$ K for a mean field CDW or SDW transition temperature. Below $T_c \approx 1.8$ K the material is a superconductor [19]. The properties of the 24 K transition are not consistent with CDW (or SDW) gap formation, and in any case, the small value of T_X permits the NFL ARPES line shape to be studied from T_X to nearly $10T_X$, a temperature high enough that any putative q-1D CDW fluctuations should be absent. Comparing the data to the theoretical Luttinger liquid line shape, we identify significant similarities, but also find important differences.

Single-crystal samples were grown by the electrolytic reduction technique [15]. The ARPES was performed at the Ames/Montana beam line of the Synchrotron Radiation Center at the University of Wisconsin. Samples oriented by Laue diffraction were mounted on the tip of a helium refrigerator and cleaved *in situ* at a temperature of 30 K just before measurement in a vacuum of

 0031-9007/99/82(12)/2540(4)$15.00

$\approx 4 \times 10^{-11}$ torr, exposing a clean surface containing the crystallographic c and q-1D b axes. Monochromatized photons of $h\nu = 24$ eV were used to obtain the spectra reported here. All the data are normalized to the photon flux. The instrumental resolution ΔE and E_F were calibrated with a reference spectrum taken on a freshly sputtered Pt foil. ΔE was 150 meV for the E_F intensity map and 50 meV for the energy distribution curves (EDC's). The angular resolution for the spectrometer was $\pm 1°$, which amounts to $\pm 7\%$ of the distance from Γ to Y in the Brillouin zone. The **k** space near-E_F intensity map was made by detecting electrons over the range $\Delta E = 150$ meV, centered 50 meV below E_F, and sweeping analyzer angles along two orthogonal directions relative to the sample normal, in steps of 1° for one angle and 2° for the other. Following standard photoemission theory [20], (i) such sweeps move the **k** vector on a spherical surface with a radius which depends on the kinetic energy and hence on the photon energy, (ii) one then observes the intersection of this spherical surface and the FS, (iii) the photohole momentum components parallel to the surface (k_x and k_y) are determined unambiguously by the analyzer angles and the kinetic energy of the photoelectron, and (iv) we have used a standard ansatz of free photoelectron bands, offset by an inner potential to which we give a nominal value of 10 eV, to deduce the perpendicular photohole momentum (k_z).

Figure 1(a) shows the projection onto the $\mathbf{k}_\parallel$ plane of our near-E_F intensity map made at a temperature of 30 K by varying both analyzer angles for fixed $h\nu = 24$ eV. Γ-Y and Γ-X are the b^* and c^* directions, respectively. Figure 1(b) shows the projection onto the $k_\perp/\Gamma$-Y plane of a map made at 200 K by fixing one analyzer angle, while varying the other angle and also the photon energy. The spherical arcs for each photon energy are easily seen, and an arrow shows the arc corresponding to the fixed photon energy of the map of Fig. 1(a). The straightness of the FS segments in both maps shows that this material fulfills very well the band theory prediction of being q-1D [21,22]. The Fermi wave vector k_F defined by the center of the left-hand FS segment is $2k_F \approx 0.57$ Å^{-1}, somewhat larger than the band theory [21,22] value of 0.51 Å^{-1}. Bright spots occur where the ARPES matrix element is large.

Figure 2(a) shows a sequence of spectra taken at 200 K $\approx 8T_X$ along a line 0.06 Å^{-1} below an X-M Brillouin zone boundary and passing through the FS at one of the bright points, as indicated in Fig. 1(a). Over the corresponding k range along Γ-Y, the calculation of Fig. 2(b) shows two bands merging and crossing E_F together. We identify the two dispersing peaks of Fig. 2(a) with these two bands, since both the calculation and our q-1D FS image show that the two bands disperse very weakly along Γ-X. The calculated bands which do not cross E_F are very weak for the special path of Fig. 2(a), but can still be seen as a small peak or general humping ~400 meV below E_F in spectra 4 to 11. These

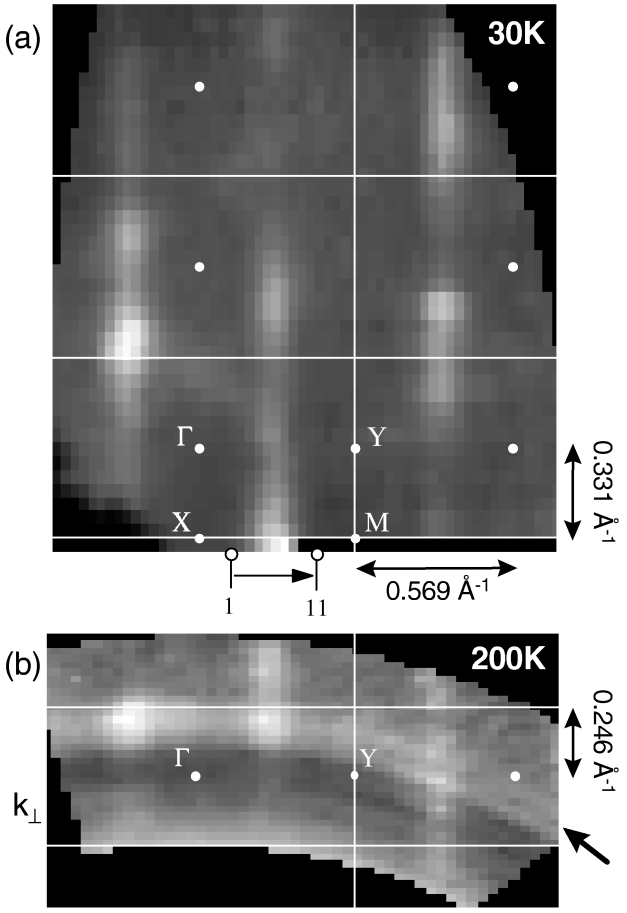

FIG. 1. Near-E_F intensity map of $Li_{0.9}Mo_6O_{17}$. (a) $k_\parallel$ plane projection for $h\nu = 24$ eV with variation of two detector angles. (b) $k_\perp/\Gamma$-Y plane projection for varying $h\nu = 15$–32 eV and one detector angle. The thick arrow in (b) indicates the arc corresponding to $h\nu = 24$ eV used in (a). In both maps, image contrast has been enhanced by dividing the data by the data heavily smoothed to retain only slowly varying cross-sectional dependences.

bands are easily seen in other spectra, e.g., along Γ-X and Γ-Y. Thus, apart from a bandwidth difference seen also for other bronzes [10,23], we find a good general agreement with band theory. Since LL models assume linear dispersion around E_F, it is noteworthy that this aspect of the band theory is observed over an energy range of 200 meV for one band and 500 meV for the other. Figure 3(a) shows the spectra overplotted so as to display the detailed line shape of the dispersing peak which defines the FS. In spectra 2 through 5 one sees the leading edge increase to a certain limit, "the wall," and in spectra 5 through 10 one sees the intensity fall, first without a change in the leading edge, and then accompanied by a shift of the leading edge away from E_F. Within the experimental resolution, very little intensity develops at E_F in any spectrum. A set of spectra taken at 50 K are identical with respect to all these features.

In the absence of any LL line shape theory including interactions between two bands, we apply line shapes

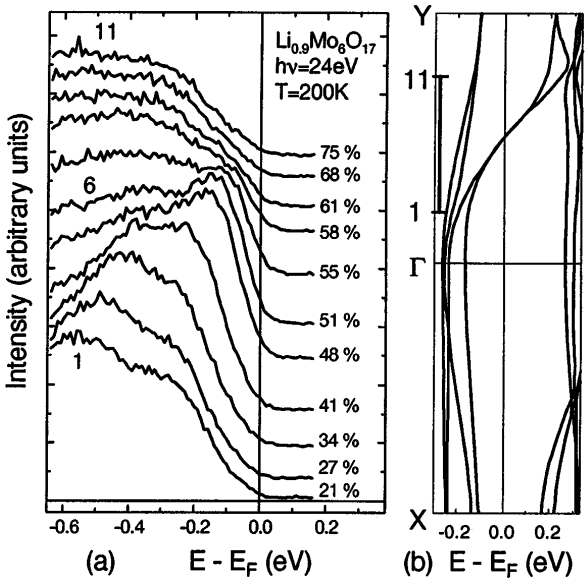

FIG. 2. (a) ARPES spectra showing FS crossing along the path, marked with an arrow in Fig. 1(a), that passes through the bright spot of the image. For each spectrum, the corresponding momentum value parallel to ΓY is given in percentage of the length of ΓY. (b) Tight binding band calculation [21] showing bands along X-Γ-Y. The bar shows the range of $k_{\Gamma Y}$ explored in (a).

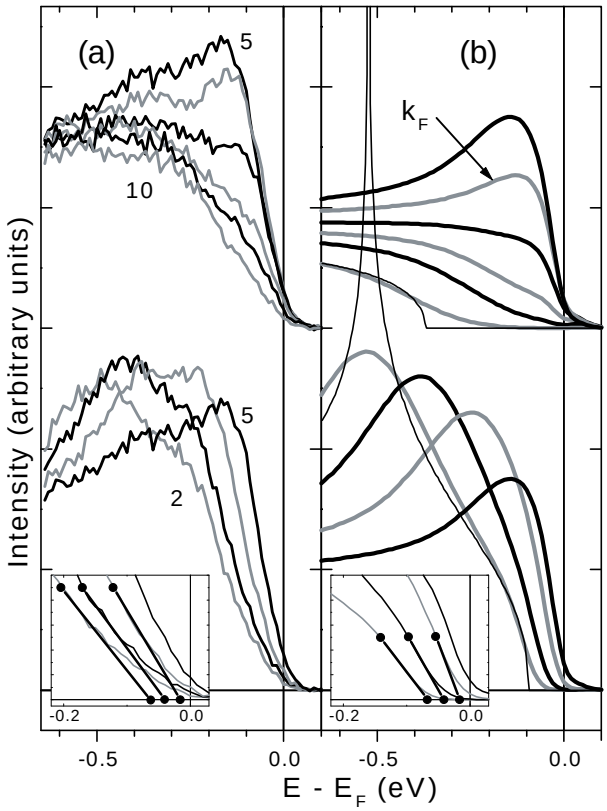

FIG. 3. (a) Spectra of Fig. 2(a) replotted to emphasize the "wall" behavior, described in text. Inset shows a detailed view of the spectral line shape approaching E_F, with lines drawn to emphasize a hint of 1D onset behavior. (b) Tomonaga-Luttinger (TL) model spectra, calculated to be compared with (a), as described in text. Inset shows the spinon edge singularity onsets.

calculated for the one-band Tomonaga-Luttinger (TL) model to the two degenerate bands crossing E_F. Figure 3(b) shows TL line shapes for a spin independent repulsive interaction [4] and singularity index $\alpha = 0.9$. The thick lines are spectra including our angle and energy resolutions. The thin lines accompanying two of the spectra show the purely theoretical curves without including the experimental resolutions. The k values and format are exactly the same as for Fig. 3(a). Before discussing the considerable similarity to the experimental data for the behavior of the leading edge, we first describe the generic theoretical features. The LL has no single particle excitations, and the removal or addition of an electron results entirely in the generation of combinations of collective excitations of the spin and charge densities, known as spinons and holons, respectively. In this TL model the spinon dispersion is that of the underlying band, $v_F k$ with Fermi velocity v_F, and the holon dispersion is $\beta v_F k$ where β depends on α and is >1. For the lower group of spectra, with k inside the FS, there is an edge singularity onset at a nonzero low energy and then a rise to a power law singularity peak at higher energies. These sharp features are greatly broadened by the experimental resolutions and, except for the slight shoulder of curve 2, the spinon features of the theory curves are simply the leading edges of the line shapes. The movements with k of the low energy onset and of the peak reflect the dispersions of the spinons and holons, respectively. That the onset occurs at a nonzero energy for $k \neq k_F$ is a direct consequence of the restrictive kinematics of 1D. For the four lowest members of the upper set of curves, k lies outside the FS. The k dependence of the nonzero singular energy onset in this case reflects the holon dispersion.

We now discuss the choice of parameters and the comparison to experiment, for which we associate the spectral peaks with the rapidly dispersing holon features and the leading edges with the slowly dispersing spinon features. We consider a range of $\alpha > 1/2$ because for $\alpha < 1/2$ the low-energy edge singularity takes the form of a peak which is obviously not present in the data. Each α determines a β and v_F is chosen so that $\beta v_F k$ matches the experimental peak movements, linear to $\approx$500 meV below E_F for one peak, but only $\approx$200 meV below E_F for the other, so that the lowest energy peak in data curves 1 to 3 has no theoretical counterpart. One finds that for the broadened spectra, as α increases from $1/2$, (a) the peak maximum as k approaches k_F decreases more rapidly, and (b) the amount of E_F weight relative to the spectrum maximum in the $k = k_F$ spectrum decreases. As expected in the TL theory [3,4], we have observed a power law onset at E_F in a measurement of the angle-integrated photoemission spectrum, from which we deduce $\alpha \approx 0.6$, nicely greater than $1/2$. For $\alpha = 0.6$

($\beta = 4$) the behavior of (a) is similar to experiment but the value for (b) is about twice the experimental value of $\approx$16%. For $\alpha = 0.9$ ($\beta = 5$), it is noticeable that the behavior of (a) is faster than in experiment, but the fractional amount of E_F weight for the $k = k_F$ spectrum is only slightly greater than in experiment. With the choice $\alpha = 0.9$ and $\hbar v_F = 0.7$ eV Å [24], the theory curves reproduce semiquantitatively the variation of the leading edge in spectra 2 to 5, the wall behavior in spectra 5 to 7, the loss of a peaky upturn at E_F from spectrum 6 to 7 as k passes beyond k_F, and qualitatively the movement of the leading edge away from E_F for spectra 8 to 10. The agreement of the intercepts given by the straight line extrapolations shown in the two insets indicates a remnant in the data of the theoretical onset behavior of 1D kinematics, and even a semiquantitative agreement with the β value linking the spinon and holon dispersions. The value of $2k_F = 0.59$ Å^{-1} from spectrum 6 may be a better value than that deduced from our FS map.

Looking in more detail, differences can be seen. First, considering the insets of Fig. 3, the amount of experimental weight in the energy range from E_F to the theory onset definitely exceeds that for the corresponding broadened theory curve. This could reflect the ultimate 3D character of the material relaxing the restrictive 1D kinematics, consistent with the increasing magnitude of the disagreement as **k** moves further from the FS and the available phase space increases. We also report that the only difference between the spectra at 200 and 50 K is a subtle change at lower temperature such that the leading edge extrapolates more to E_F. This presently tentative finding might hint at a departure from LL behavior towards increased 3D character as T moves closer to the phase transition at T_X. In any case, we note that gap loss with decreasing T is opposite to the behavior expected [6] for the case of a pseudogap associated with gap formation (e.g., CDW or SDW) at T_X. Second, the magnitude of the edge movement for experimental spectra 8 to 10 is much less than in the theory, probably due to the interfering presence in the spectra of the contributions from the two bands further below E_F. Thus the detailed differences can plausibly be attributed to the oversimplifications of the TL model, e.g., its one-band nature and its strict 1D character, relative to the experimental situation. The fact that our α value is much larger than the value $1/8$ for the 1D Hubbard model could also be a consequence of some 3D coupling [25].

To conclude, the spectra reported are currently unique in showing the line shape of the dispersing excitation which defines the FS for interacting electrons in a q-1D non-CDW metal. Although there are important differences in detail, there is a remarkable similarity to the line shape of the TL model of the LL. Characteristic features of the TL model line shape originate in the underlying charge-spin separation of the LL scenario. Previous ARPES reports [26] of charge-spin separation have been for q-1D materials where a Mott-Hubbard insulator precludes the LL. This is the first such report for a q-1D metal.

Work at UM was supported by the U.S. Department of Energy (DoE) under Contract No. DE-FG02-90ER45416 and by the U.S. National Science Foundation (NSF) Grant No. DMR-94-23741. Work at the Ames Lab was supported by the DoE under Contract No. W-7405-ENG-82. The Synchrotron Radiation Center is supported by the NSF under Grant No. DMR-95-31009.

*Department of Physics, National Chang-Hua University of Education, Chang-Hua 50058, Taiwan, Republic of China.

[1] P. W. Anderson, Phys. Rev. Lett. **64**, 1839 (1990); **65**, 2306 (1990).
[2] F. D. M. Haldane, J. Phys. C **14**, 2585 (1981).
[3] J. Voit, Phys. Rev. B **47**, 6740 (1993).
[4] V. Meden and K. Schönhammer, Phys. Rev. B **46**, 15 753 (1992).
[5] P. A. Lee *et al.*, Phys. Rev. Lett. **31**, 462 (1973).
[6] R. H. McKenzie and D. Scarratt, Phys. Rev. B **54**, R12 709 (1996).
[7] B. Dardel *et al.*, Phys. Rev. Lett. **67**, 3144 (1991).
[8] B. Dardel *et al.*, Europhys. Lett. **24**, 687 (1993).
[9] R. Claessen *et al.*, J. Electron Spectrosc. Relat. Phenom. **76**, 121 (1995); J. W. Allen *et al.*, J. Phys. Chem. Solids **56**, 1849 (1995).
[10] G.-H. Gweon *et al.*, J. Phys. Condens. Matter **8**, 9923 (1996).
[11] F. Zwick *et al.*, Phys. Rev. Lett. **79**, 3982 (1997).
[12] K. E. Smith *et al.*, Phys. Rev. Lett. **70**, 3772 (1993).
[13] M. Grioni *et al.*, Phys. Scr. **T66**, 172 (1996).
[14] K. Breuer *et al.*, J. Vac. Sci. Technol. A **12**, 2196 (1994); The beam line has a negligible amount of 2nd order light of energy higher than $\sim$35 eV, due to its low energy grating.
[15] C. Schlenker *et al.*, Physica (Amsterdam) **135B**, 511 (1985).
[16] Y. Matsuda *et al.*, J. Phys. C **19**, 6039 (1986).
[17] For examples, see G. Travaglini and P. Wachter, Phys. Rev. B **30**, 1971 (1984) (CDW); L. Degiorgi *et al.*, Phys. Rev. Lett. **76**, 3838 (1996) (SDW).
[18] L. Degiorgi *et al.*, Phys. Rev. B **38**, 5821 (1988).
[19] M. Greenblatt *et al.*, Solid State Commun. **51**, 671 (1984).
[20] F. J. Himpsel, Adv. Phys. **32**, 1 (1983).
[21] M.-H. Whangbo and E. Canadell, J. Am. Chem. Soc. **110**, 358 (1988).
[22] Reference [12] found larger dispersion perpendicular to the sample surface than we do and a different $2k_F \approx 0.7$ Å^{-1}. Both differences can be attributed to our better resolution of the near-E_F peak which defines the FS.
[23] G.-H. Gweon *et al.*, Phys. Rev. B **55**, R13 353 (1997).
[24] For the large k,ω range of the linear dispersion, the universal spectral function used here is valid if the potential range parameter $r_c < 0.7$ Å [4]. The r_c dependence is then too weak to discern in the comparison to the data and we conservatively chose $r_c = 0.1$ Å.
[25] P. Kopietz *et al.*, Phys. Rev. Lett. **74**, 2997 (1995).
[26] C. Kim *et al.*, Phys. Rev. Lett. **77**, 4054 (1996); H. Fujisawa *et al.*, Solid State Commun. **106**, 543 (1998).